MNRAS **000**, 1–7 (2018) Preprint 17 April 2018 Compiled using MNRAS LATEX style file v3.0

Cosmic Variance in Binary Population Synthesis

Katelyn Breivik,[1,2]★ Shane L. Larson,[1,2]
[1]*Department of Physics and Astronomy, Northwestern University, 2145 Sheridan Road, Evanston, IL 60208, USA*
[2]*Center for Interdisciplinary Exploration and Research in Astrophysics (CIERA), Northwestern University, 2145 Sheridan Road, Evanston, IL 60208, USA*

Accepted XXX. Received YYY; in original form ZZZ

ABSTRACT

The most numerous source for space-based gravitational wave observatories are kilosecond period compact binaries in the Milky Way. These systems will be visible to LISA throughout the galaxy, and will contribute to a limiting astrophysical foreground below ∼1 mHz. Some constraints on the number and character of these systems exist from surveys of the nearby volume of the galaxy, but most of our assumptions about what LISA will observe are inferred from full population simulations. Galactic population simulation efforts generally focus on high fidelity models that require extensive computational power to produce a single simulated population for each model. Each simulated population represents an incomplete sample of the functions governing compact binary evolution, thus introducing variance from one simulation to another. We present a rapid Monte-Carlo population simulation technique that can simulate thousands of populations in less than a week, thus allowing a full exploration of the variance associated with a binary stellar evolution model. In the context of considering the capabilities of a gravitational wave observatory, this will expand our ability to assess the likely scenarios that LISA will encounter when it begins observations of the galaxy. Once LISA has obtained a catalog of compact binary observations, population synthesis can be used for model comparison studies to better understand the physical models for the formation and evolution of compact binary populations.

Key words: binaries: close – gravitational waves – methods: statistical

1 INTRODUCTION

Binary systems containing stellar remnants are the most prolific source class for both ground and space-based gravitational-wave (GW) observatories. To date the Laser Interferometer Gravitational Wave Observatory (LIGO) has detected the inspiral and merger of five binary black holes (BBHs) and one binary neutron star (BNS) Abbott, B. P. et al (2016a); Abbott, B. P. et al. (2016b, 2017a,b,c); Abbott et al. (2017). The Laser Interferometer Space Antenna (*LISA*) is expected to observe the population of $\sim 10^7$ binary stellar remnants, or compact binaries, in the Milky Way and its surrounding environment forming a confusion foreground of gravitational radiation in the millihertz region of the gravitational wave spectrum . Of these 10^7 binaries, $\sim 10,000$ are expected to be resolved above the foreground, offering a unique probe of the populations of stellar remnants in the local Universe Amaro-Seoane et al. (2017).

Simulations of the Galactic compact binary populations are useful in understanding the astrophysical power that comes with a space-based gravitational wave detector like *LISA* . Several population synthesis investigations using different stellar evolution codes (e.g. Hils et al. 1990; Nelemans et al. 2001b; Ruiter et al. 2010; Yu & Jeffery 2013; Liu & Zhang 2014; Korol et al. 2017; Lamberts et al. 2018), have considered how galactic compact binary populations are affected by different binary evolution models (e.g. common envelope evolution, metallicity dependent stellar winds, etc.), initial population conditions (e.g. stellar initial mass function (IMF), binary separation and eccentricity), and star formation histories (SFHs)).

Generally, each study seeks to determine which physical processes are most important in shaping the detection catalog and astrophysical foreground for a *LISA* -like observatory. To this end, in each study a single galactic population and its detection catalog are simulated for a single model or a set of several models that canvas the available parameter space. Consequently, current studies are missing an understanding of the range of possible galactic populations that *LISA* might observe as a consequence of statistical fluctuations, or 'cosmic variance,' that affect the both the intrinsic

★ E-mail: katelynbreivik2013@u.northwestern.edu

(e.g. binary) and extrinsic (e.g. position) parameters contained the *LISA* detection catalog.

We present COSMIC (Compact Object Synthesis and Monte-Carlo Investigation Code), a Monte-Carlo binary population synthesis code that generates large compact binary populations from which many galactic population realizations can be Monte-Carlo sampled. Simulated *LISA* detection catalogs from the sampled galactic realizations can then inform the range of possible galactic compact binary populations detectable by *LISA* . This is especially important when considering populations with low numbers, such as the subset of mass transferring double white dwarfs (DWDs) with helium accretors observable by *LISA and Gaia* , which is expected to contain *dozens* of systems rather than hundreds or thousands (Kremer et al. 2017; Breivik et al. 2018).

There are currently a wide range of uncertainties in what stellar evolutionary physics is important in defining the properties of the Milky Way stellar population. There are already several tools in place with varying levels of resolution and focus, including, SeBa (Portegies Zwart & Verbunt 1996; Nelemans et al. 2001a; Toonen et al. 2012), BSE, (Hurley et al. 2002), StarTrack (Belczynski et al. 2002, 2008), binary_c (Izzard et al. 2004, 2006, 2009), and SEVN (Spera et al. 2015), that provide flexibility to explore different aspects of stellar and binary evolution. While binary evolution is currently implemented in COSMIC using BSE, COSMIC is agnostic with respect to the underlying population synthesis code used as its generator. The COSMIC framework can be integrated with different population synthesis codes that use different stellar evolution prescriptions, provided their output is written to a standard format.

The paper is organized as follows. In Sec. 2 we summarize the key features of COSMIC . We detail the additional binary evolution prescriptions that have been added to the version of BSE used in COSMIC in Sec. 3. In Sec. 4 we demonstrate the capabilities of COSMIC to produce a reference population of compact binaries observable by *LISA* . We finish with a discussion in Sec. 5.

2 OVERVIEW: COSMIC

There are two main outputs from COSMIC : (1) the fixed population, a collection of binary systems that has enough constituents to capture the underlying shape of the population's parameter distribution functions resulting from a given star formation history (SFH) and binary evolution model, (2) Monte-Carlo-sampled galactic realizations, which can be used to explore the variance in synthetic catalogs associated with a given galactic population and binary evolution model. In this paper, we explore the variance associated with the Milky Way compact binary populations, made up of combinations of WDs, NSs, and BHs, that will be observable by LISA.

The general process to simulate a set of synthetic catalogs is as follows:

(i) Generate an initial population based on user-selected models for Milky Way SFH and initial binary parameter distributions

(ii) Evolve the initial population to it's state at present day following the user-specified SFH

(iii) Compare the total population to the population made on the previous step and ask whether or not the shape of the parameter distribution has changed significantly (we introduce a quantitative 'match' condition for making this assessment, described in Sec 2.1)

(iv) If the match has not converged, repeat from step 1, adding the new population to the previous population

(v) If the match has converged, the population is called the 'fixed population' – a large enough sample to contain the esential statistical features of a fully evolved pop synthesis model.

(vi) Monte-Carlo sample Galactic realizations of the population from a multi-dimension KDE fit to the fixed population

Each compact binary population (e.g. helium WD - carbon-oxygen WD) can simulated separately, or as a group (e.g. all double WDs), and the time to generate a fixed population ranges from the order of hours to days depending on the shape of each population, with unimodal parameter distributions converging faster than multi-modal distributions. The simulation time to generate the multidimensional KDE and sample 100 galactic realizations for a binary population is on the order of several hours to a few days, depending on the number of sources expected to be in the galactic population. Figure 1 illustrates the structure and process COSMIC uses to generate populations.

2.1 Fixed population

Since COSMIC is designed to generate discrete synthetic Galactic catalogs, we evolve each population according to a SFH for the specific galaxy we are interested in. Thus, to generate a 'Milky Way fixed population', we evolve populations for each epoch of star formation over the age of the Milky Way while tracking the physical properties of the population (including compact object births and mergers, as well as binary parameters) as a function of time. The fixed population is simulated once for each combination of SFH and binary evolution model; thus a study with ten binary evolution models and one SFH will have ten associated fixed populations. Galactic realizations can then be Monte-Carlo sampled to generate a statistical set of synthetic catalogs for each model (i.e. a full study with ten binary evolution models and one SFH will contain *one thousand* synthetic catalogs).

The demonstration of COSMIC presented in this paper implements binary evolution using the binary stellar evolution code BSE, with several modifications including updated common envelope, wind, and kick prescriptions which are described further in Sec. 3.

Regardless of binary evolution model, the fixed population is generated from an initial population of binaries sampled from distribution functions to assign each binary with an initial metallicity (Z), primary mass (m), mass ratio (q), orbital separation (a), eccentricity (e), and birth time (T_0) according to a given star formation history. Since binary evolution codes generally simulate a single binary at a time, initial binary populations can be generated using several different star formation histories and distribution functions.

COSMIC is currently equipped to generate initial populations according to several binary parameter distributions.

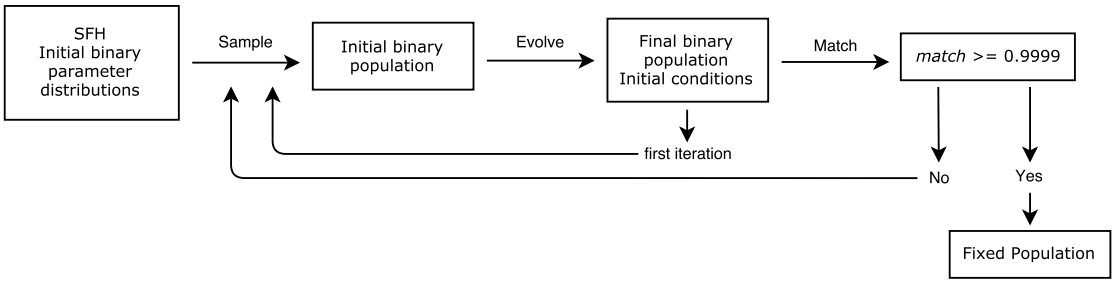

Figure 1. Schematic for the process `COSMIC` uses to generate a fixed population. Generally, the process moves from left to right. The quantities in the first box are provided by the user. Once a Fixed Population is generated, Milky Way realizations can be Monte-Carlo sampled to generate realistic synthetic Galacitc catalogs. See also the list of steps outlined above in Section 2

If the parameters are treated independently, initial masses may be sampled from both a Salpeter (1955) or Kroupa et al. (1993) initial mass function (IMF); mass ratios are uniformly sampled (Mazeh et al. 1992; Goldberg & Mazeh 1994); orbital separations are sampled according to Han (1998); eccentricities are sampled from a thermal distribution (Heggie 1975); binarity can be assumed to have user specified fractions or the mass-dependent fraction of van Haaften et al. (2013). `COSMIC` is also designed to generate initial binary samples from the Moe & Di Stefano (2017) multi-dimensional binary parameter distributions, which include mass and separation dependent binary fractions.

`COSMIC` is currently equipped to generate populations according to very simple star formation history prescriptions. For a more detailed study on the effect of star formation history, see Lamberts et al. (2018). We assume the thin disk formed through constant star formation over the last 10 Gyr and the that bulge and thick disks formed through bursts of star formation lasting 1 Gyr and occurring 10 Gyr and 11 Gyr in the past respectively Robin et al. (2003). We assume $Z = Z_{\odot}$ for all systems in the thin disk and bulge and $Z = 0.15\,Z_{\odot}$ for systems in the thick disk Yoshii (2013).

There is no formulaic way to *a priori* predict the required number of binaries to be evolved for a fixed population, since each fixed population depends on a different binary evolution model. The ideal number of simulated systems in a fixed population is such that the population adequately describes the final parameter distribution functions while not simulating so many systems as to be inefficient. To quantify this number, we apply a *match* criteria, based on matched filtering and template matching techniques, to histograms of binary parameter data from our simulated populations.

We use independently generated histograms for each binary parameter, with binwidths determined using Knuth's Rule (Knuth 2006) implemented in `astropy` (Astropy Collaboration et al. 2013), to track the distribution of each parameter as successive populations are simulated and cumulatively added to the fixed population. Before each histogram is generated, we ensure that similar binwidths are used for each parameter as well as enforce the physical limits of the simulated systems (e.g. positive definite values for mass and orbital period and eccentricities between 0 and 1) by transforming into log space as necessary.

We define the *match* as

$$match = \frac{\sum_{k=1}^{N} P_{k,i} P_{k,i+1}}{\sqrt{\sum_{k=1}^{N} (P_{k,i} P_{k,i}) \sum_{k=1}^{N} (P_{k,i+1} P_{k,i+1})}}, \quad (1)$$

where $P_{k,i}$ denotes the probability for the k^{th} bin for the i^{th} iteration. The *match* is limited to values between 0 and 1 and tends to unity as the parameter distributions converge to a distinct shape.

Binary systems are evolved until $match > 0.9999$ for all binary parameters of interest or the change in the *match* for any binary parameter between successively simulated populations is $< 10^{-6}$. Figure 2.1 illustrates how the primary mass distribution for DWDs with a Thin Disk star formation history evolves as systems are successively added to the population. In this population, the resolution of the peaks at orbital periods of ~ 10 yr and $\sim 10^{-4}$ yr are important tracers of two different formation channels for DWDs. We note that in panel (a) of Figure 2.1, the peak at $\sim 10^{-4}$ yr is poorly resolved, while it is better resolved in panels (b) and (c). We also note that there is very little change in the distribution shape of panels (b) and (c), illustrating why it is appropriate to require a $match > 0.9999$ but not higher.

The peak at 10 yr is exclusively populated by pairs of carbon-oxygen WDs, with the majority of systems having undergone a common envelope evolution between an asymptotic-giant-branch (AGB) star and a carbon-oxygen WD that results in their present orbital period. Changes to the common envelope efficiency and binding energy of the AGB star's envelope can both shift this peak to different orbital periods as well as change the relative height of the peak.

The 10^{-4} yr peak is populated by pairs of combinations of helium WDs and carbon-oxygen WDs, where the majority of the systems undergo two common envelope episodes. In this case, the second common envelope contains a WD and a giant-branch star and results in a very short orbital period that falls within the region of LISA's sensitivity. As with the peak at 10 yr, changes to common envelope evolution prescriptions can lead to shifts in both the location and height of the peak. Understanding the landscape of how different common envelope prescriptions change this population may lead to the opportunity for LISA observations to constrain the elusive common envelope physics.

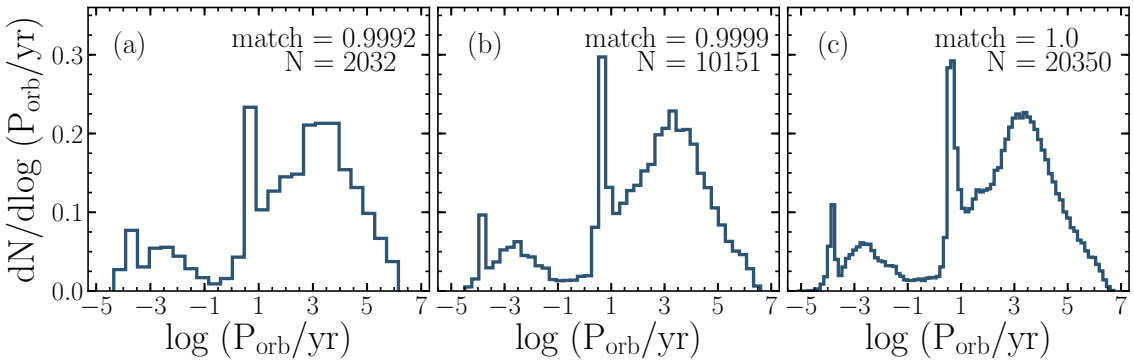

Figure 2. The orbital period distribution of a Milky Way thin disk DWD population. Panels (a), (b), and (c) show how the distribution shape changes as more DWD binaries are simulated and added to the population. The number of systems in the population and *match* is shown in the upper right corner of each panel. Note the two peaks, at 10 yr and 10^{-4} yr, are the result of two formation channels, both involving the common envelope phase, that produce an excess of systems at a particular orbital period. Resolving peaks like these provides an important insight in the processes which shape the population.

2.2 Generating Monte-Carlo population realizations

Once the fixed population satisfies our match criteria, we generate a multi-dimensional Gaussian kernel density estimate (KDE) for the parameters with computed *matches*. The multi-dimensional KDE accounts for any correlations between the binary parameters and represents the probability for a each combination of binary parameters for a given population. We choose the KDE bandwidth to be the minimum binwidth of the histograms generated for the final *match* criteria. Note that the KDEs are generated for the *transformed* data, so that a single bandwidth selection is still appropriate.

For each galactic realization, we Monte-Carlo sample N_{bin} sets of binary parameters from the fixed population as well as three dimensional galactic positions and the inclination (i), argument of periapsis (ω), and longitude of ascending nodes (Ω) for each system. The total number of systems, N_{bin}, in a given galactic realization is determined by the number of systems formed in the fixed population normalized to the ratio of the total mass of the galactic component and the total mass, including single and binary systems, of the fixed population.

We adopt galactic position distributions and galactic component masses from McMillan (2011) as a fiducial model. We assume the mass in the thin and thick disks to be $4.32\times10^{10}\,M_\odot$ and $1.44\times10^{10}\,M_\odot$ respectively. We assume the mass of the bulge to be $8.9\times10^{9}\,M_\odot$. We distribute systems in the thin and thick disks as:

$$\rho(R,z) \propto \exp\big[-R/R_0 - z/z_0\big], \tag{2}$$

where $R_{0,\rm thin} = 2.9\,$kpc, $z_{0,\rm thin} = 0.3\,$kpc and $R_{0,\rm thick} = 3.31\,$kpc, $z_{0,\rm thick} = 0.9\,$kpc. We distribute systems in the bulge as:

$$\rho(r') \propto (1 + r'/r_0)^{-1.8} \exp\big[-(r'/r_{\rm cut})^2\big], \tag{3}$$

where

$$r' = \sqrt{R^2 + (z/q)^2} \tag{4}$$

and $r_0 = 0.075\,$kpc, $r_{\rm cut} = 2.1\,$kpc, and $q = 0.5$. We also note that COSMIC can not only be used to study Galactic population physics, but also the implication of the galactic model and the influence of scale heights on derived catalogs by changing these parameterizations.

3 UPDATES TO BSE

While `COSMIC` is designed to be agnostic to the choice of binary evolution prescriptions and population synthesis codes, in the current release, stellar evolution and binary interactions are implemented through the binary evolution code: `BSE`. The version of `BSE` currently used by `COSMIC` uses several upgrades which are consistent with the binary stellar evolution prescriptions of Rodriguez et al. (2016) which were updated to be comparable to the models and detailed in Dominik et al. (2013). We briefly describe the upgrades below.

The `BSE` stellar wind prescriptions have been amended to include metallicity dependent winds for O and B stars as well as Wolf-Rayet stars. The winds for O and B stars are treated according to the prescription of Vink et al. (2001), which considers stars with temperatures $12,500\,\mathrm{K} < T_{\rm eff} < 22,500\,\mathrm{K}$ and $27,500\,\mathrm{K} < T_{\rm eff} < 50,000\,\mathrm{K}$ separately. As in Rodriguez et al. (2016), we adopt the methods of Dominik et al. (2013) where the high and low temperature prescriptions are extended to $T_{\rm eff} = 25,000\,\mathrm{K}$. Wolf-Rayet stars are treated according to Vink & de Koter (2005).

Two new prescriptions for the supernova mechanism have been added to following Fryer et al. (2012), which account for material falling back onto the compact objects formed in core-collapse supernovae which are both convection enhanced and neutrino driven. The two cases are delineated by the time between core bounce and explosion, with a 'rapid' explosion which only allows for explosions which occur within 250 ms and a 'delayed' explosion which allows for longer timescales to explosion. The main difference in these two prescriptions is the presence of a mass gap between neutron stars and black holes which is produced in the rapid case, but not present in the delayed case. With the inclusion of fallback onto compact objects, the natal kick prescriptions of `BSE` have been updated to account for reduced natal kick

magnitudes due to the fraction of ejected mass during the supernova that falls back onto the compact object.

We have also added the Xu & Li (2010) prescription which computes the binding energy parameter (λ) to be used in the common envelope prescription. This prescription accounts for different stellar evolutionary stages and masses by simulating a grid of stars between $1\,M_\odot$ and $20\,M_\odot$ for metallicities $Z = 0.02$ and $Z = 0.001$. As a fiducial common envelope model, we use the variable binding energy parameter in conjunction with a constant common envelope efficiency parameter $\alpha = 1.0$ following previous results (e.g. Nelemans et al. 2001a; Dominik et al. 2012). However, we also note that previous studies of post-common-envelope binaries, suggest that the efficiency may be as low as $\alpha = 0.2$ (Zorotovic et al. 2010; Toonen & Nelemans 2013; Camacho et al. 2014).

We emphasize here that methods outlined in Sec. 2 are *independent* of the implementation of stellar evolution and binary interactions. Thus, `COSMIC` can be easily adapted to include binary evolution prescriptions or entirely new binary evolution codes as they are released.

4 A FIDUCIAL MILKY WAY GALAXY FOR LISA

As an illustration of the capabilities of `COSMIC`, we simulate the population of binaries containing combinations of white dwarfs (WDs), neutron stars (NSs), and black holes (BHs) with orbital periods $10\,\mathrm{s} < \mathrm{P_{orb}} < 10^5\,\mathrm{s}$. As a fiducial binary evolution model we implement the prescriptions described in § 3, specifically choosing the 'rapid' supernova mechanism prescription. Otherwise, we implements the defaults in the original `BSE` code release.

As described in §2, we simulate a population for each of the Milky Way mass components: the thin and thick disks and the bulge. We assume masses and spatial distributions following McMillan (2011). We assume a four year LISA observation time. We compute the S/N of each system as:

$$(S/N)^2 = 2\,T_{\rm obs} \sum_n \left(\frac{h_n^2}{S_n(nf)}\right), \tag{5}$$

where

$$h_n = 8\frac{G}{c^2}\frac{M_c}{D}\left(\frac{G}{c^3}\pi f_0 M_c\right)^{2/3}\frac{\sqrt{g(n,e)}}{n}. \tag{6}$$

In the equations above, $T_{\rm obs}$, $\mathcal{M}_c = (M_1 M_2)^{3/5}/((M_1 M_2)^{3/5})^{1/5}$ is the chirp mass, f_0 is the orbital frequency, D is the distance, and $g(n,e)$ is the Peters (1964) factor that accounts for GW emission of an eccentric binary. We use Cornish & Robson (2018) to estimate the LISA sensitivity for an observation time of 4 yr.

Table 1 shows a summary of the number of sources per population and Milky Way component, as well as the number of systems for LISA signal to noise ratio: S/N > 7 from 100 Milky Way population realizations. We choose this S/N since binary systems with S/N > 7 are expected to be resolved as individual sources above the foreground signal of the Galactic population.

We find that the vast majority of the population of resolved compact binaries is comprised of DWD systems. We note that the thick disk is the only Galactic component that contains resolved binaries containing a BH, while binary NS systems are only expected to be resolved from the thin disk population. Our findings are broadly consistent with most previous work (e.g. Hils et al. 1990; Nelemans et al. 2001b; Ruiter et al. 2010; Yu & Jeffery 2013; Liu & Zhang 2014; Korol et al. 2017), with the exception of Lamberts et al. (2018), which predicts one resolvable binary BH. The main differences in our predicted catalogs and previous works arise from differences in both binary evolution models as well as Galactic component masses and spatial distributions. We emphasize, however, that while different studies will consider different assumptions, the strength of `COSMIC` is the ability to simulate a several different models and a large number of synthetic catalogs to investigate these differences.

The root power spectral density (rPSD) of our 100 Milky Way population realizations, along with the LISA sensitivity curve, is plotted in Figure REF. We down sample the LISA observation time by a factor of 50 so that each

Table 1. Summary of 100 Milky Way population realizations

Component	Binary Population	$\mathrm{N_{total}}$	$\mathrm{N_{ave}}$ S/N > 7
Thin Disk	WD-WD	3.23×10^8	6.97×10^4
	NS-WD	1.02×10^7	1.38×10^4
	BH-WD	3.62×10^5	0
	NS-NS	1.07×10^6	52
	NS-BH	6.62×10^3	0.2
	BH-BH	3.65×10^6	0
Thick Disk	WD-WD	1.44×10^8	1.48×10^4
	NS-WD	3.13×10^6	29
	BH-WD	5.31×10^5	0
	NS-NS	3.19×10^3	0
	NS-BH	1.12×10^5	23
	BH-BH	2.14×10^6	34
Bulge	WD-WD	1.75×10^8	3.33×10^3
	NS-WD	4.04×10^6	1.37×10^3
	BH-WD	3.62×10^5	0
	NS-NS	1.65×10^4	0.3
	NS-BH	1.72×10^5	0
	BH-BH	1.02×10^6	0
	Total	6.69×10^8	1.03×10^5

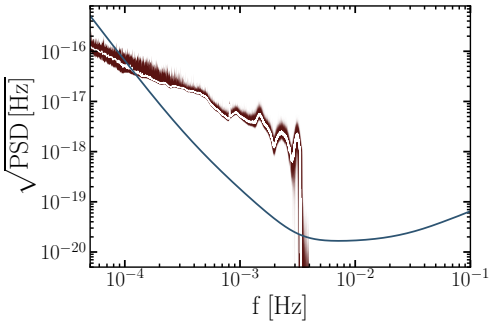

Figure 3. The root power spectral density as a function of GW frequency from 100 Milky Way population realizations is shown in red with a LISA sensitivity curve plotted in blue. The red region shows the $99_{\rm th}$ percentile confidence limits while the solid white line shows the $50_{\rm th}$ percentile from the populations.

frequency bin has binwidth $bw = 50/T_{\rm obs} = 3.96 \times 10^{-7}$ Hz. The solid white line and shaded red region shows the $50_{\rm th}$ percentile and $99_{\rm th}$ percentile confidence limits from our populations. The vast majority of the signal in the rPSD is due to the population of DWDs. The characteristic shape, especially the fall off near 1 mHz, is due to the number of systems radiating GWs in a given frequency bin. At low frequencies the number of sources per bin is high both because most sources preferentially have longer orbital periods and because the number of bins is low when compared with the number of bins at higher frequencies. This leads to a higher likelihood of a source occupying its own frequency bin at frequencies in excess of 1 mHz.

The features present in the rPSD are often smoothed out to produce a DWD foreground, e.g. Littenberg et al. (2013); Korol et al. (2017). Here, we present the unsmoothed rPSD in order to illustrate the variance in potential rPSDs LISA might observe as well as highlight the interesting structure produced from the population. This structure is largely due to the distribution of orbital periods and masses produced the binary evolution model we used to generate the populations. Different binary evolution models will produce different rPSDs, thus providing an avenue to distinguish between different binary evolution models. The ability to describe how the rPSD varies from realization to realization is especially important since we expect the general shape to stay constant from model to model. In order to properly determine which models LISA can constrain, the variance in potential rPSDs needs to be explored to confirm which features are present in spite of the variance.

Another benefit to simulating many Milky Way population realizations is the ability to investigate how small subsets of each population vary from realization to realization. Figure 4 plots the chirp mass, orbital period, and distance distributions for the 500 highest S/N systems for each of our population realizations. The solid lines so the $50_{\rm th}$ percentile from the realizations and the shaded regions show the $99_{\rm th}$ percentile confidence regions. While the overall distribution shape is well defined, understanding the extent of the variance that arises from the combination of the 'intrinsic' parameters (e.g. $\mathcal{M}_c$ and $P_{\rm orb}$ and 'extrinsic' parameters (e.g. D) aids in comparisons between binary evolution models.

5 DISCUSSION

We have presented a new binary population synthesis code, `COSMIC` , whose goal is rapidly to produce a statistical set of realistic Milky Way compact binary populations. We have detailed the process `COSMIC` uses to produce it's two major outputs: the fixed population and Milky Way realizations. As an illustrative example, we have simulated 100 Milky Way realizations of the thin disk, thick disk, and bulge for all combinations of double compact objects potentially observable by LISA. We find $\sim 10^5$ systems that are expected to be observed by LISA, after a 4 yr observation time, with $S/N > 7$.

Future studies using `COSMIC` to self consistently explore the resolved populations of several binary evolution models as well as Galactic component formation histories and spatial distribution. These studies will provide important necessary insights into the populations containing NSs and BHs which will be important in comparing to current and future LIGO results. Furthermore, as future electromagnetic observations produce new compact-binary catalogs, the binary evolution models can be adapted to best represent the compact binary population of the Milky Way.

ACKNOWLEDGEMENTS

The majority of our analysis was performed using the computational resources of the Quest high performance computing facility at Northwestern University which is jointly supported by the Office of the Provost, the Office for Research, and Northwestern University Information Technology.

REFERENCES

Abbott, B. P. et al 2016a, Phys. Rev. Lett., 116, 061102
Abbott, B. P. et al. 2016b, Phys. Rev. Lett., 116, 241103
Abbott, B. P. et al. 2017a, Phys. Rev. Lett., 118, 221101
Abbott, B. P. et al. 2017b, Phys. Rev. Lett., 119, 141101
Abbott, B. P. et al. 2017c, Phys. Rev. Lett., 119, 161101
Abbott B. P., et al., 2017, ApJ, 851, L35
Amaro-Seoane P., et al., 2017, preprint, (arXiv:1702.00786)
Astropy Collaboration et al., 2013, A&A, 558, A33
Belczynski K., Kalogera V., Bulik T., 2002, ApJ, 572, 407
Belczynski K., Kalogera V., Rasio F. A., Taam R. E., Zezas A., Bulik T., Maccarone T. J., Ivanova N., 2008, ApJS, 174, 223
Breivik K., Kremer K., Bueno M., Larson S. L., Coughlin S., Kalogera V., 2018, ApJ, 854, L1
Camacho J., Torres S., García-Berro E., Zorotovic M., Schreiber M. R., Rebassa-Mansergas A., Nebot Gómez-Morán A., Gänsicke B. T., 2014, A&A, 566, A86
Cornish N., Robson T., 2018, preprint, (arXiv:1803.01944)
Dominik M., Belczynski K., Fryer C., Holz D. E., Berti E., Bulik T., Mandel I., O'Shaughnessy R., 2012, ApJ, 759, 52
Dominik M., Belczynski K., Fryer C., Holz D. E., Berti E., Bulik T., Mandel I., O'Shaughnessy R., 2013, ApJ, 779, 72
Fryer C. L., Belczynski K., Wiktorowicz G., Dominik M., Kalogera V., Holz D. E., 2012, ApJ, 749, 91
Goldberg D., Mazeh T., 1994, A&A, 282, 801
Han Z., 1998, MNRAS, 296, 1019
Heggie D. C., 1975, MNRAS, 173, 729
Hils D., Bender P. L., Webbink R. F., 1990, ApJ, 360, 75
Hurley J. R., Tout C. A., Pols O. R., 2002, MNRAS, 329, 897
Izzard R. G., Tout C. A., Karakas A. I., Pols O. R., 2004, MNRAS, 350, 407
Izzard R. G., Dray L. M., Karakas A. I., Lugaro M., Tout C. A., 2006, A&A, 460, 565
Izzard R. G., Glebbeek E., Stancliffe R. J., Pols O. R., 2009, A&A, 508, 1359
Knuth K. H., 2006, ArXiv Physics e-prints,
Korol V., Rossi E. M., Groot P. J., Nelemans G., Toonen S., Brown A. G. A., 2017, MNRAS, 470, 1894
Kremer K., Breivik K., Larson S. L., Kalogera V., 2017, ApJ, 846, 95
Kroupa P., Tout C. A., Gilmore G., 1993, MNRAS, 262, 545
Lamberts A., et al., 2018, preprint, (arXiv:1801.03099)
Littenberg T. B., Larson S. L., Nelemans G., Cornish N. J., 2013, MNRAS, 429, 2361
Liu J., Zhang Y., 2014, PASP, 126, 211
Mazeh T., Goldberg D., Duquennoy A., Mayor M., 1992, ApJ, 401, 265
McMillan P. J., 2011, MNRAS, 414, 2446
Moe M., Di Stefano R., 2017, ApJS, 230, 15

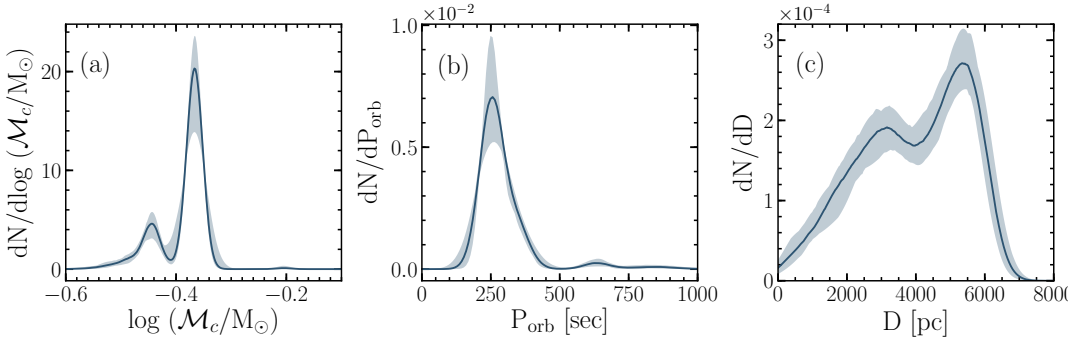

Figure 4. Distributions of the chirp mass, orbital period and distance of the 500 loudest resolved sources from 100 Milky Way realizations. The solid lines show the 50_{th} percentile from the realizations while the shaded regions show the 99_{th} percentile confidence limits. The general distribution shapes are well defined, but the confidence limits show small variations in the location and height of each peak and trough in the distributions.

Nelemans G., Yungelson L. R., Portegies Zwart S. F., Verbunt F., 2001a, A&A, 365, 491
Nelemans G., Yungelson L. R., Zwart S. F. P., 2001b, A&A, 375, 890
Peters P. C., 1964, Physical Review, 136, 1224
Portegies Zwart S. F., Verbunt F., 1996, A&A, 309, 179
Robin A. C., Reylé C., Derrière S., Picaud S., 2003, A&A, 409, 523
Rodriguez C. L., Chatterjee S., Rasio F. A., 2016, PhysRevD, 93, 084029
Ruiter A. J., Belczynski K., Benacquista M., Larson S. L., Williams G., 2010, ApJ, 717, 1006
Salpeter E. E., 1955, ApJ, 121, 161
Spera M., Mapelli M., Bressan A., 2015, MNRAS, 451, 4086
Toonen S., Nelemans G., 2013, A&A, 557, A87
Toonen S., Nelemans G., Portegies Zwart S., 2012, A&A, 546, A70
Vink J. S., de Koter A., 2005, A&A, 442, 587
Vink J. S., de Koter A., Lamers H. J. G. L. M., 2001, Rev. Mex. Astron. Astrofis., 369, 574
Xu X.-J., Li X.-D., 2010, ApJ, 716, 114
Yoshii Y., 2013, Star Counts and Nature of the Galactic Thick Disk. p. 393, doi:10.1007/978-94-007-5612-0_8
Yu S., Jeffery C. S., 2013, Mon. Not. R. Astron. Soc., 429, 1602
Zorotovic M., Schreiber M. R., Gänsicke B. T., Nebot Gómez-Morán A., 2010, A&A, 520, A86
van Haaften L. M., Nelemans G., Voss R., Toonen S., Portegies Zwart S. F., Yungelson L. R., van der Sluys M. V., 2013, A&A, 552, A69

This paper has been typeset from a TEX/LATEX file prepared by the author.